Acta Oncologica, 2010; 49: 906–913

informa
healthcare

ORIGINAL ARTICLE

Non-invasive imaging of combretastatin activity in two tumor models: Association with invasive estimates

THOMAS NIELSEN[1,2], RUMI MURATA[1], ROSS J. MAXWELL[3], HANS STØDKILDE-JØRGENSEN[4], LEIF ØSTERGAARD[2], CARSTEN D. LEY[5], PAUL E. G. KRISTJANSEN[5] & MICHAEL R. HORSMAN[1]

[1]*Department of Experimental Clinical Oncology, Aarhus University Hospital, Aarhus, Denmark,* [2]*Department of Neuroradiology, Center of Functionally Integrative Neuroscience, Aarhus University Hospital, Aarhus, Denmark,* [3]*University of Newcastle Upon Tyne, Northern Institute for Cancer Research, Newcastle upon Tyne, UK,* [4]*MR Research Centre, Aarhus University Hospital, Aarhus, Denmark and* [5]*Department of Biomedical Sciences, University of Copenhagen, Copenhagen, Denmark*

Abstract

Introduction. The efficacy of the vascular disrupting agent combretastatin A-4 phosphate (CA4P) depends on several factors including tumor size, nitric oxide level, interstitial fluid pressure, and vascular permeability. These factors vary among tumor types. The aim of this study was to investigate all these factors in two tumor models that respond differently to CA4P. *Material and methods.* Mice bearing C3H mammary carcinomas or KHT sarcomas (200 to 800 mm^3) were intraperitoneally injected with CA4P (100 mg/kg). Tumor size and the effect of a nitric oxide inhibitor nitro-L-arginine (NLA) administered intravenously were evaluated by necrotic fraction histologically assessed at 24 hours. Interstitial fluid pressure (IFP) was measured using the wick-in-needle technique, and vascular characteristics were assessed with dynamic contrast-enhanced magnetic resonance imaging (DCE-MRI). *Results.* Initial necrotic fraction was about 10% in both tumor models at 200 mm^3, but only increased significantly with tumor size in the C3H mammary carcinoma. In this tumor, CA4P significantly induced further necrosis by about 15% at all sizes, but in the KHT tumor, the induced necrotic fraction depended on tumor size. For both tumor types, NLA with CA4P significantly increased necrotic fraction above that for each drug alone. CA4P significantly decreased IFP in all tumors except in the 800 mm^3 C3H tumor, which had an initially non-significant lower value. Interstitial volume estimated by DCE-MRI increased in all groups, except the 800 mm^3 C3H tumors. DCE-MRI vascular parameters showed different initial characteristics and general significant reductions following CA4P treatment. *Conclusions.* Both tumor models showed differences in all factors before treatment, and in their response to CA4P. Perfusion and permeability as estimated by DCE-MRI play a central role in the CA4P response, and interstitial volume and IFP seemed related. These factors may be of clinical value in the planning of CA4P treatments.

The tubulin binding agent combretastatin A-4 phosphate (CA4P) is a leading vascular disrupting agent (VDA) in clinical trials [1]. It has cytotoxic and antiproliferative effects against dividing endothelial cells and thereby induces vascular damage and perfusion changes in various tumor types. Its efficacy, however, varies significantly among different tumor types [2]. Moreover, regardless of the degree of vascular damage, the drug has only a small impact on tumor growth [3,4]; it is general for VDAs that a substantial effect is seen in central tumor regions, whereas peripheral tumor cells, that obtain their nutrient supply from the surrounding tissue's physiological vessels, are unaffected by the treatment [3] and form a viable rim.

Factors have been identified which influence the effect of CA4P. Insight into the mechanisms behind these influences may allow modification of these factors in order to improve the efficacy of CA4P. Tumor size is one factor; CA4P and other VDAs show a tumor size dependent anti-tumor effect [5,6], and the degree of necrosis induced by CA4P treatment

Correspondence: Thomas Nielsen, Department of Experimental Clinical Oncology, Aarhus University Hospital, Nørrebrogade 44, Building 5, DK-8000 Aarhus C, Denmark. Tel: +45 89492627. Fax: +45 86197109. E-mail: thomas@oncology.dk

(Received 19 May 2010; accepted 29 May 2010)

ISSN 0284-186X print/ISSN 1651-226X online © 2010 Informa Healthcare
DOI: 10.3109/0284186X.2010.499135

depends on both tumor model and size [2]. Another factor is the endogenous vasodilator nitric oxide (NO), which has been shown to have a protective effect against CA4P [7]. Initial interstitial fluid pressure (IFP) also influences response to tubulin binding agents. It is related with improved cell survival following treatment with ZD6126 [8], and in a study of the tubulin stabilizer patupilone, it predicted tumor response as measured using a tumor volume endpoint, and correlated positively with vascularity and negatively with apoptosis [9]. Another study has also shown a correlation between vessel permeability and the response to CA4P [10]. Factors, which are affected by VDA treatment have also been identified. These are important in the investigation of VDA mechanisms, and they could play an important role when combining VDAs with other treatments. IFP has been shown to decrease following treatment with VDAs [8,9,11], while vascular permeability has been shown to increase [12–14]. Vascular permeability has also been assessed non-invasively by dynamic contrast-enhanced magnetic resonance imaging (DCE-MRI) [10,15–20], but the factors estimating permeability are also influenced by other factors [16,21], and they are often decreased following VDA treatment. DCE-MRI has also become a promising tool for treatment optimization [22–27].

Although understanding the factors that influence response to VDAs may lead to improvements in activity, VDAs are still unlikely to be applied as stand alone treatments. More likely, they will be used in combination with other more conventional treatments. Radiation therapy and chemotherapy suffer from low efficacy in hypoxic tumor regions, which often appear in neovascularized central tumor areas. CA4P is believed to increase the effect of these treatments by acting on these neovascularized regions. For example, the combination of VDAs with radiation therapy has been investigated with promising results [1–3, 28–30]. Information on IFP and vascularity, which are affected by VDA treatment, may be important for optimizing timing and doses in such combinations.

All the above mentioned factors related to CA4P activity have been investigated in different studies using different tumor models, but to our knowledge, no study has investigated all of these factors in the same tumor models. The aim of this study was to investigate tumor size, NO level, interstitial fluid pressure, and DCE-MRI parameters in two tumor models previously shown to respond differently to CA4P with focus on the information obtainable by *in vivo* imaging.

Material and methods

Animal and tumor model

C3H mammary carcinomas grown in female CDF_1 mice and KHT sarcomas grown in female C3H/km mice were used for all experiments. Derivation and maintenance of the tumor models have been described previously [31,32]. All tumors were implanted into the right rear foot of the animals. Experiments were performed when tumors had reached 200 to 800 mm^3 in size, which typically occurred three to four weeks after inoculation. Tumor volume was calculated from the formula $D1 \times D2 \times D3 \times \pi/6$, where the D values represent the three orthogonal diameters. All experiments were performed under national and European Union-approved guidelines for animal welfare.

Drug preparation

CA4P was supplied by OXiGENE, Inc. (Waltham, MA, USA). The drug was dissolved in saline immediately prior to each experiment; it was kept cold and protected from light. The stock solution was further diluted in saline so that it could be given as a single intraperitoneal (i.p.) injection at a constant volume of 0.02 ml/g at a dose of 100 mg/kg mouse body weight. Nitro-L-arginine (Sigma Chemical Co., St. Louis, MO, USA) (NLA) was dissolved in saline and administered intravenously (i.v.) at a dose of 10 mg/kg in a volume of 0.02 ml/g mouse body weight.

Necrotic fraction

Mice were sacrificed by cervical dislocation 24 h after i.p. injection of CA4P and their tumors excised. They were then fixed in formalin, and hematoxylin and eosin stained sections were made. For each tumor a randomly selected section was cut and the two additional, equally spaced sections (400 μm apart) were produced and examined under a projecting microscope. Each section was systematically scanned and projected on a grid with 60 equidistant-spaced points. For each field of vision, the total number of points overlying tumor (nT) and necrosis (nN) were recorded, and necrotic fraction of the tumor was defined by $\Sigma nN/\Sigma nT$. Necrotic fractions were compared by Student's t-test or two-way analysis of variance (ANOVA) with $p<0.05$ considered significant.

Interstitial fluid pressure

Prior to the IFP experiments, mice were anesthetized by a subcutaneous injection of 0.3 ml xylazine (Rompun; Bayer Healthcare, Kgs. Lyngby, Denmark) and ketamine (Ketalar; Pfizer, Sollentuna, Sweden) diluted 1:4:15 in isotonic normal saline. The mice were restrained in specially constructed lucite jigs. The tumor-bearing legs were then exposed and loosely attached to the jig with tape without impairing the blood supply to the foot. IFP was measured

using the wick-in-needle technique [33] with small modifications [34], using a 23 G side-holed needle with a 2 mm side-hole. The sensing needle was coupled to a pressure sensor by a water column in 0.58 mm hosing (inner diameter). The pressure sensor was connected to a MacLab/4e (ADInstruments Ltd., Australia) through a ML112 bridge amplifier (ADInstruments Ltd., Australia). Pressure data from the sensor were collected from the MacLab/4e digitizer by the SCSI interface using a PC with PowerLab® Chart software v. 4.2 (ADInstruments Ltd., Australia). The pressure sensing system was calibrated against a water column of predefined height prior to each experiment, and calibration was checked at the end of each experiment. Calibration remained stable over time. A total of three identical pressure measurement setups were connected to the MacLab, so that the IFP of three tumors could be measured independently at the same time. IFP values were compared by Student's t-test with $p<0.05$ considered significant.

Dynamic contrast enhanced MRI

A 7 Tesla spectroscopy/imaging system (Varian, Palo Alto, CA, USA) was used for the DCE-MRI. Non-anesthetized mice were restrained with the tumor-bearing legs exposed as described for the IFP experiments. An i.v. line was applied in a tail vein for administration of the contrast agent Gd-DTPA (Magnevist, Schering, Berlin, Germany), and an i.p. line was inserted for administration of CA4P. The mice were scanned before and three hours following CA4P treatment.

The semiquantitative parameter initial area under the curve (IAUC) was calculated, and the standard DCE-MRI model including a vascular term was applied for quantitative estimation of the transfer constant, K^{trans}, the rate constant, k_{ep}, the extravascular extracellular space, $v_e = K^{trans}/k_{ep}$, and the plasma volume fraction, v_p [21]. The imaging protocol and data analysis are reported previously [19]. Pre- and post-treatment parameter maps were compared with respect to median values of identical ROIs by one-way ANOVA with $p<0.05$ considered significant.

Results

Tumor size

The two tumor models both showed initial necrotic fractions of about 10% (see Figure 1). Increasing tumor size caused necrotic fraction to increase linearly with the logarithm of the tumor size in the C3H mammary carcinoma (significant differences between all sizes except 500 and 800 mm^3). In the KHT sarcoma, necrotic fraction did not increase with tumor size. Treatment with CA4P significantly increased necrotic fraction with an almost fixed amount (about 15% of the tumor volume) at all sizes in the C3H mammary carcinoma. In the KHT sarcoma, the treatment induced no further necrosis at 200 mm^3, but at 300 mm^3 and above, necrotic fraction increased significantly and size-dependently to a level at 800 mm^3 comparable to that seen in the C3H mammary carcinoma at this size.

Nitric oxide

Figure 2 shows that NLA alone had little or no effect on necrotic fraction at 24 h in both tumors, and CA4P significantly increased the necrotic fraction in the C3H mammary carcinoma only (Student's t-test, $p=0.008$). The effect on necrotic fraction was greatest when combining the drugs, it appeared to lead to significantly greater effects than either agent alone in both tumor models at all times. A two-way ANOVA

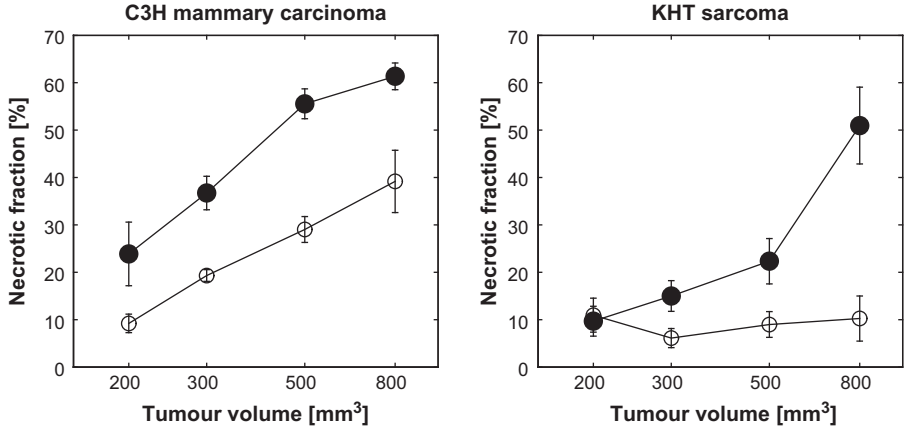

Figure 1. Necrotic fraction versus logarithmic tumor size for control animals (○) and animals treated with 100 mg/kg i.p. CA4P (●). Measurements were performed 24 hours following treatment. Left: C3H mammary carcinoma, right: KHT sarcoma. Results show mean (± 1 SE) for 6–18 mice/group.

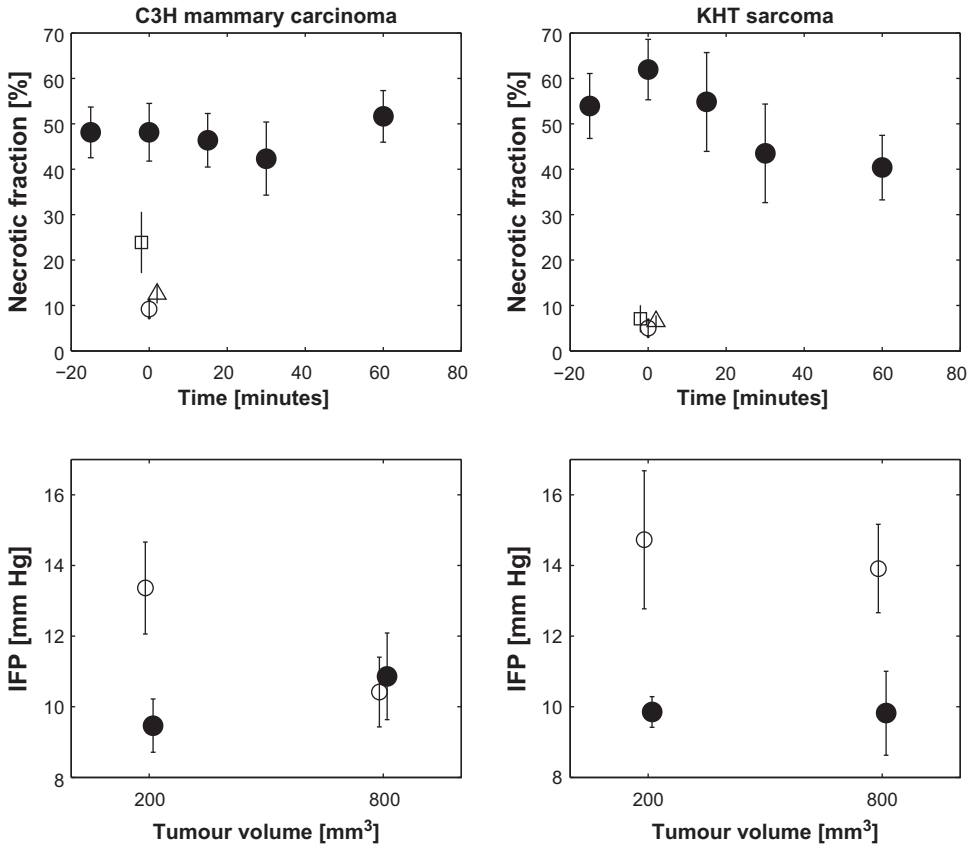

Figure 2. Upper panel: Necrotic fraction measured 24 hours following no treatment (○), treatment with 10 mg/kg i.v. NLA alone (Δ), 100 mg/kg i.p. CA4P alone (□), or treatment with both NLA and CA4P (●). For the combined treatment, measurements were performed 24 hours following CA4P administration, and the abscissa shows the time point of NLA administration relative to the administration of CA4P, which was given at time point 0. Lower panel: Interstitial fluid pressure versus tumor size for control animals (○) and animals treated with 100 mg/kg i.p. CA4P 3 hours prior to the measurement (●). Left panels: C3H mammary carcinoma, right panels: KHT sarcoma. Results show mean (± 1 SE) for 6–18 mice/group.

with interaction showed a statistical interaction between CA4P and NLA when they were given together ($p=0.016$). The effect of administration time of NLA relative to CA4P appeared to be slightly different in the two tumors; in the KHT sarcoma, the necrotic fractions after administering NLA either at the same time or 60 minutes after CA4P were significantly different (Student's t-test, $p=0.045$) with the largest effect when the drugs were given simultaneously. In the C3H mammary carcinoma, there was no dependence of necrotic fraction on the investigated intervals between administration of the two drugs.

Interstitial fluid pressure

The measurements of IFP are also shown in Figure 2. Initial IFP in the 200 mm^3 C3H mammary carcinoma dropped significantly ($p=0.014$) after treatment. In the 800 mm^3 C3H mammary carcinoma, the initial IFP was lower (although not significantly) and did not change after treatment. For the KHT sarcoma, initial IFP values at the two sizes were similar and decreased significantly to the same level ($p<0.05$). These IFP values for the KHT sarcoma pre- and post-CA4P treatment matched those for the 200 mm^3 C3H mammary carcinoma. Thus, the C3H mammary carcinoma differed from the KHT sarcoma by showing a size dependency for IFP. An additional observation is that CA4P decreases IFP in tumors exhibiting larger IFP values.

DCE-MRI

The DCE-MRI results are shown in Table 1 and Figure 3. The interstitial volume, v_e, non-significantly increased to comparable levels in all treatment groups except the 800 mm^3 C3H mammary carcinoma, where v_e did not increase. The 800 mm^3 C3H mammary carcinoma also differed in the IFP results, where IFP did not decrease as in all other groups. This suggests a relationship between the CA4P induced changes in interstitial pressure and volume.

Table 1. DCE-MRI results.

	Initial DCE-MRI values (mean ± 1 SE)			
	C3H 200 mm^3 (n=7)	C3H 800 mm^3 (n=6)	KHT 200 mm^3 (n=8)	KHT 800 mm^3 (n=8)
IAUC [10^{-3}Ms]	15.3 ± 1.03	11.6 ± 2.05	11.7 ± 1.69	11.5 ± 1.18
K^{trans} [$10^{-3}s^{-1}$]	0.389 ± 0.0405	0.418 ± 0.0893	0.637 ± 0.0891	0.678 ± 0.0702
k_{ep} [$10^{-3}s^{-1}$]	4.15 ± 0.311	2.95 ± 0.317	5.57 ± 0.744	5.12 ± 0.354
v_e [%]	8.84 ± 0.976	11.9 ± 1.12	13.2 ± 3.89	11.4 ± 0.977
v_p [%]	4.58 ± 0.386	3.70 ± 0.697	3.14 ± 0.503	2.5 ± 0.328
	Relative change in DCE-MRI values in % (mean ± 1 SE)			
	C3H 200 mm^3	C3H 800 mm^3	KHT 200 mm^3	KHT 800 mm^3
IAUC	–42.3 ± 8.99	–48.5 ± 5.45	–41.8 ± 10.4	–45.2 ± 10.3
K^{trans}	–26.8 ± 9.31	–55.0 ± 10.0	–43.3 ± 12.4	–61.2 ± 6.83
k_{ep}	–30.8 ± 7.54	–31.4 ± 7.75	–57.1 ± 9.13	–52.4 ± 9.44
v_e	23.3 ± 9.30	–8.48 ± 5.19	32.8 ± 12.9	23.0 ± 11.0
v_p	–58.1 ± 11.9	–59.1 ± 13.2	–58.9 ± 13.1	–57.2 ± 18.0

The other DCE-MRI parameters shown are all related to vasculature. The semiquantitative vascular parameter IAUC indicated a higher initial vascularization in the 200 mm^3 C3H mammary carcinoma than in all other groups (not significant) and showed reduction with comparable changes in all tumors. However, the IAUC reductions were only statistically significant in the 200 mm^3 C3H mammary carcinoma and the 800 mm^3 KHT sarcoma ($p<0.01$). The model parameters of plasma volume, v_p, and K^{trans}, the latter depending on blood flow and permeability surface area product, showed some further differences. Comparing all C3H mammary carcinomas and all KHT sarcomas, the C3H mammary carcinoma generally had a higher v_p ($p=0.010$), whereas the KHT sarcoma had a higher K^{trans} ($p=0.002$). Following treatment, both K^{trans} and v_p were significantly reduced in all tumor groups. v_p was reduced with comparable changes, but comparing all 200 mm^3 tumors and all 800 mm^3 tumors, K^{trans} showed a significant ($p=0.028$) size dependency with the largest change in the large tumors.

Discussion

Tumor size played different roles in the two tumor models. In the C3H mammary carcinoma, necrotic fraction increased with tumor size, but it was independent of size in the KHT sarcoma. This could possibly be explained by differences in vascularity between the tumor models. Intuitively, the vascular characteristics of the KHT sarcoma prevents increases in necrotic fraction with increasing tumor size. The vascular differences between the tumor models found by DCE-MRI were higher plasma volume (v_p) in the C3H mammary carcinoma and higher K^{trans} in the KHT sarcoma. K^{trans} and v_p, however, did not change with tumor size in any of the tumors. The higher K^{trans} in the KHT sarcoma indicates higher blood flow or permeability surface area product, so

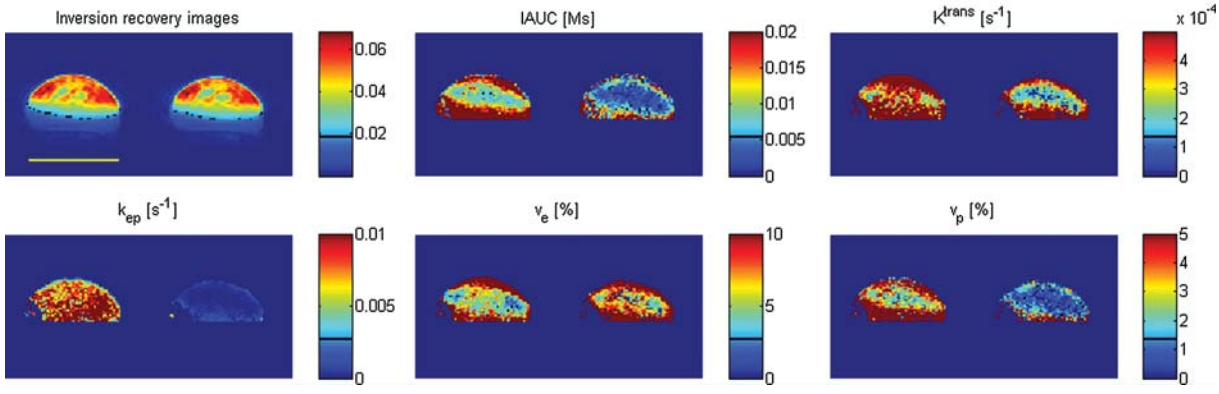

Figure 3. Example of images (inversion recovery with $T_I=2400$ ms) and parameter maps produced by kinetic analysis: IAUC, K^{trans}, k_{ep}, v_e, and v_p. The images are produced for the same 200 mm^3 KHT sarcoma before (left) and 3 hours after treatment with CA4DP (right). On the inversion recovery images, the light blue color shows the leg visible to the left of the tumor and the foot below the tumor, and the yellow line indicates 1 cm. The images and maps show intratumor heterogeneity and overall reduction of the vascular parameters IAUC, K^{trans}, k_{ep}, and v_p.

one of these quantities is assumed to explain the differences in necrotic fraction.

The CA4P induced change in necrotic fraction was independent of tumor size in the C3H mammary carcinoma, where necrotic fraction was increased with an almost fixed amount (about 15%) at all sizes. In the KHT sarcoma, the treatment induced no further necrosis at 200 mm^3, but at 300 mm^3 and above, necrotic fraction increased significantly and size-dependently to a level at 800 mm^3 comparable to that seen in the 800 mm^3 C3H mammary carcinoma. There was no initial difference in DCE-MRI parameters between the 200 mm^3 and 800 mm^3 KHT sarcomas, which could have explained their different increase in necrotic fraction. The DCE-MRI vascular response in all tumor groups was large, but this did not show a difference, which could explain the size-dependent response of the KHT sarcomas. There was a size-dependent difference in the response of K^{trans}, but this was common for the two tumor models. The size dependency of the response in the KHT sarcoma is in accordance with the size-dependent cell survival following treatment with ZD6126 in this tumor model [6] and with the size-dependent growth delay induced by CA4P in rhabdomyosarcomas [5].

IFP has been correlated with vascularity [9], and like the vascular parameters K^{trans} and v_p, the IFP did not show any difference between the 200 mm^3 and 800 mm^3 KHT sarcomas. In the C3H mammary carcinoma, however, IFP differed between the two sizes unlike the vascular parameters. Both the initial IFP and the IFP reduction at 200 mm^3 were in accordance with the KHT sarcoma values, but at 800 mm^3 IFP was initially lower and did not change following CA4P treatment. The initially high IFP originates from an equalization to blood pressure through the highly permeable vessels and physical confinement of the tumor cells [35]. The vascular characteristics of the 800 mm^3 C3H mammary carcinoma was, however, similar to those at 200 mm^3. Besides its correlation with vascularity, initial IFP has also been correlated negatively with apoptosis [9], and therefore the cause of the initially lower IFP in the 800 mm^3 C3H mammary carcinoma may be the higher necrotic fraction. Furthermore, the lack of IFP reduction in the 800 mm^3 C3H mammary carcinoma was in accordance with a lack of increase in the interstitial volume (v_e), which was seen in the other treatment groups. Initial IFP has been shown to be predictive of response to VDAs as measured by cell survival and tumor volume [8,9], but in the C3H mammary carcinoma showing size-dependent IFP, the CA4P induced necrotic fractions were similar. The general reductions in initially high IFP values were, however, in accordance with these studies. DCE-MRI parameters have been correlated with IFP in tumors without necrotic regions [36], but such a relation was not seen in our study.

In the DCE-MRI analysis, voxels with initially low contrast uptake were assumed necrotic and omitted. This was necessary because the model analysis can not be performed in voxels with no contrast uptake, and it should therefore be kept in mind that the results are for living tissue. Voxels, which showed contrast uptake before treatment and not three hours after treatment were assumed to be living and showing complete vascular shutdown. These were included for all parameters except v_e, and the parameter values were set to 0. The reason why they were not included for v_e was the the interstitial volume could not be estimated or assumed to be 0, so this parameter was compared using only voxels with contrast uptake at both time points.

The importance of nitric oxide for vascular development has been shown by letting experimental tumors overexpress dimethylarginine dimethylaminohydrolase, which metabolizes endogenous inhibitors of NO synthesis [37]. This resulted in increased tumor blood volume and growth rate, but the vessel caliber estimated by the MRI method of vessel size imaging (VSI) in that study was not affected. NO is also used as a provascular approach to radiosensitization [38]. Previously, NO was shown to have a protective effect against CA4P [7]. NLA increased the effect of CA4P in both tumor models in the current study. Given alone, NLA has been shown to cause a 50% decrease in erythrocyte velocity by reduction of arteriolar diameter [13]. In the same study, CA4P was shown to reduce the number of small vessels. In fact, our recent study of CA4P action in the C3H mammary carcinoma by VSI also showed that the induced reduction in blood volume mainly was reduction in volume of small vessels (Nielsen et al., unpublished data). VSI has also shown a vessel size decrease following treatment with patupilone [9]. These are supposedly the mechanisms involved in the drug effects seen in this study. Reduced blood velocity caused by NLA may explain the enhancement in CA4P induced necrotic fraction. The NLA induced reduction in arteriolar diameter can increase arteriolar vascular resistance leading to a pressure drop rendering the distal capillary blood pressure lower. As blood pressure contributes to the high IFP, this blood pressure decrease may decrease IFP. High IFP is believed to reduce drug delivery by preventing convection from blood plasma to interstitium [35], and the IFP reduction could therefore enhance drug delivery. This would explain the enhancement in CA4P induced necrotic fraction. However, a recent study showed that NLA's enhancement of CA4P induced necrosis was largest when NLA was given three hours following CA4P [39]. A possible explanation may be that an initially high

perfusion followed by an NLA induced IFP reduction is optimal for the CA4P effect.

The factors influencing the response to CA4P that were measured in this study are the major factors known to have an effect. But, there are probably other factors that may play a role. One of these may be vessel maturity. Pericyte involvement with vessels is believed to be indicative of vessel maturation, and there is evidence that tumors that stain positively for the presence of pericytes are more resistant to vascular shutdown [40].

A vascular dose response of CA4P obtained by DCE-MRI in the C3H mammary carcinoma showed decreased vascular response when the drug dose exceeded a certain value [19]. It is currently being investigated whether this is related to the known side effect of hypertension, and preliminary data show that different CA4P doses increased blood pressure to the same level but for different durations (Busk et al., unpublished data). This also argues for the importance of blood pressure, which in this case is caused by the drug itself. Besides the impact on drug delivery through IFP increase, hypertension may force blood flow through vessels, which otherwise would be shut down.

Conclusions

The two tumor models investigated in this study showed differences with respect to tumor size, NO level, IFP, and vascularity, both in the initial values obtained and in the changes seen following treatment with CA4P. Furthermore, some of the different factors appeared interrelated. The question remains as to how this information about the factors of importance for CA4P activity can be used to select patients for CA4P therapy and how such factors can be manipulated to improve CA4P activity. Performing DCE-MRI scans before and after CA4P treatment, as was done in some of the phase I clinical studies [41–43] would certainly provide information as to how a patient would respond to CA4P. These patients that do not respond could then have their NO levels monitored and an NO inhibitor applied where necessary.

Acknowledgements

The authors would like to thank Ms. Inger Marie Horsman, Ms. Dorthe Grand, Ms. Pia Schjerbeck, and Mr. Mogens J. Johannsen for excellent technical assistance. Supported by the Danish Cancer Society, the Danish Research Agency, and CIRRO - The Lundbeck Foundation Center for Interventional Research in Radiation Oncology and The Danish Council for Strategic Research.

Declaration of interest: Michael R. Horsman is consultant for OXiGENE. The authors alone are responsible for the content and writing of the paper.

References

[1] Horsman MR, Siemann DW. Pathophysiologic effects of vascular-targeting agents and the implications for combination with conventional therapies. Cancer Res 2006;66:11520–39.

[2] Murata R, Siemann DW, Overgaard J, Horsman MR. Interaction between combretastatin A-4 disodium phosphate and radiation in murine tumors. Radiother Oncol 2001;60: 155–61.

[3] Chaplin DJ, Pettit GR, Hill SA. Anti-vascular approaches to solid tumour therapy: Evaluation of combretastatin A4 phosphate. Anticancer Res 1999;19:189–95.

[4] Horsman MR, Murata R. Combination of vascular targeting agents with thermal or radiation therapy. Int J Radiat Oncol Biol Phys 2002;54:1518–23.

[5] Landuyt W, Verdoes O, Darius DO, Drijkoningen M, Nuyts S, Theys J, et al. Vascular targeting of solid tumours: A major 'inverse' volume-response relationship following combretastatin A-4 phosphate treatment of rat rhabdomyosarcomas. Eur J Cancer 2000;36:1833–43.

[6] Siemann DW, Rojiani AM. The vascular disrupting agent ZD6126 shows increased antitumor efficacy and enhanced radiation response in large, advanced tumors. Int J Radiat Oncol Biol Phys 2005;62:846–53.

[7] Parkins CS, Holder AL, Hill SA, Chaplin DJ, Tozer GM. Determinants of anti-vascular action by combretastatin A-4 phosphate: Role of nitric oxide. Br J Cancer 2000;83: 811–6.

[8] Skliarenko JV, Lunt SJ, Gordon ML, Vitkin A, Milosevic M, Hill RP. Effects of the vascular disrupting agent ZD6126 on interstitial fluid pressure and cell survival in tumors. Cancer Res 2006;66:2074–80.

[9] Ferretti S, Allegrini PR, O'Reilly T, Schnell C, Stumm M, Wartmann M, et al. Patupilone induced vascular disruption in orthotopic rodent tumor models detected by magnetic resonance imaging and interstitial fluid pressure. Clin Cancer Res 2005;11:7773–84.

[10] Beauregard DA, Hill SA, Chaplin DJ, Brindle KM. The susceptibility of tumors to the antivascular drug combretastatin A4 phosphate correlates with vascular permeability. Cancer Res 2001;61:6811–5.

[11] Hori K, Saito S. Microvascular mechanisms by which the combretastatin A-4 derivative AC7700 (AVE8062) induces tumour blood flow stasis. Br J Cancer 2003;89:1334–44.

[12] Ferrero E, Villa A, Ferrero ME, Toninelli E, Bender JR, Pardi R, et al. Tumor necrosis factor alpha-induced vascular leakage involves PECAM1 phosphorylation. Cancer Res 1996;56:3211–5.

[13] Tozer GM, Prise VE, Wilson J, Cemazar M, Shan S, Dewhirst MW, et al. Mechanisms associated with tumor vascular shut-down induced by combretastatin A-4 phosphate: Intravital microscopy and measurement of vascular permeability. Cancer Res 2001;61:6413–22.

[14] Kim JH, Lew YS, Kolozsvary A, Ryu S, Brown SL. Arsenic trioxide enhances radiation response of 9L glioma in the rat brain. Radiat Res 2003;160:662–6.

[15] Robinson SP, McIntyre DJO, Checkley D, Tessier JJ, Howe FA, Griffiths JR, et al. Tumour dose response to the antivascular agent ZD6126 assessed by magnetic resonance imaging. Br J Cancer 2003;88:1592–7.

[16] Evelhoch JL, LoRusso PM, He Z, DelProposto Z, Polin L, Corbett TH, et al. Magnetic resonance imaging measurements of the response of murine and human tumors to the vascular-targeting agent ZD6126. Clin Cancer Res 2004;10: 3650–7.
[17] Zhao D, Jiang L, Hahn EW, Mason RP. Tumor physiologic response to combretastatin A4 phosphate assessed by MRI. Int J Radiat Oncol Biol Phys 2005;62:872–80.
[18] Chen G, Horsman MR, Pedersen M, Pang Q, Stødkilde-Jørgensen H. The effect of combretastatin A4 disodium phosphate and 5,6-dimethylxanthenone-4-acetic acid on water diffusion and blood perfusion in tumours. Acta Oncol 2008;47:1071–6.
[19] Nielsen T, Murata R, Maxwell RJ, Stødkilde-Jørgensen H, Ostergaard L, Horsman MR. Preclinical studies to predict efficacy of vascular changes induced by combretastatin a-4 disodium phosphate in patients. Int J Radiat Oncol Biol Phys 2008;70:859–66.
[20] Nielsen T, Mouridsen K, Maxwell RJ, Stødkilde-Jørgensen H, Østergaard L, Horsman MR. Segmentation of dynamic contrast enhanced magnetic resonance imaging data. Acta Oncol 2008;47:1265–70.
[21] Tofts PS, Brix G, Buckley DL, Evelhoch JL, Henderson E, Knopp MV, et al. Estimating kinetic parameters from dynamic contrast-enhanced T(1)-weighted MRI of a diffusable tracer: Standardized quantities and symbols. J Magn Reson Imaging 1999;10:223–32.
[22] Fowler A, Forstner D, Lin P, Cuganesan R, Clark J. Multimodality imaging in the radiation treatment planning for a case of carcinoma of the nasopharynx. Acta Oncol 2008; 47:1459–60.
[23] Røe K, Muren LP, Rørvik J, Olsen DR, Dahl O, Bakke A, et al. Dynamic contrast enhanced magnetic resonance imaging of bladder cancer and implications for biological image-adapted radiotherapy. Acta Oncol 2008;47:1257–64.
[24] Søvik A, Skogmo HK, Bruland ØS , Olsen DR, Malinen E. DCEMRI monitoring of canine tumors during fractionated radiotherapy. Acta Oncol 2008;47:1249–56.
[25] Franiel T, Lüdemann L, Taupitz M, Böhmer D, Beyersdorff D. MRI before and after external beam intensity-modulated radiotherapy of patients with prostate cancer: The feasibility of monitoring of radiation-induced tissue changes using a dynamic contrast-enhanced inversion-prepared dual-contrast gradient echo sequence. Radiother Oncol 2009;93: 241–5.
[26] Seierstad T, Hole KH, Saelen E, Ree AH, Flatmark K, Malinen E. MR-guided simultaneous integrated boost in preoperative radiotherapy of locally advanced rectal cancer following neoadjuvant chemotherapy. Radiother Oncol 2009; 93:279–84.
[27] Søvik S, Skogmo HK, Andersen EKF, Bruland ØS, Olsen DR, Malinen E. DCEMRI of spontaneous canine tumors during fractionated radiotherapy: A pharmacokinetic analysis. Radiother Oncol 2009;93:618–24.
[28] Horsman MR, Murata R, Breidahl T, Nielsen FU, Maxwell RJ, Stødkiled-Jørgensen H, et al. Combretastatins novel vascular targeting drugs for improving anti-cancer therapy. Combretastatins and conventional therapy. Adv Exp Med Biol 2000;476:311–23.
[29] Murata R, Siemann DW, Overgaard J, Horsman MR. Improved tumor response by combining radiation and the vascular-damaging drug 5,6-dimethylxanthenone-4-acetic acid. Radiat Res 2001;156:503–9.
[30] Siemann DW, Warrington KH, Horsman MR. Targeting tumor blood vessels: An adjuvant strategy for radiation therapy. Radiother Oncol 2000;57:5–12.
[31] Overgaard J. Simultaneous and sequential hyperthermia and radiation treatment of an experimental tumor and its surrounding normal tissue in vivo. Int J Radiat Oncol Biol Phys 1980;6:1507–17.
[32] Kallman RF, Silini G, Putten LMV. Factors influencing the quantitative estimation of the in vivo survival of cells from solid tumors. J Natl Cancer Inst 1967;39:539–49.
[33] Fadnes HO, Reed RK, Aukland K. Interstitial fluid pressure in rats measured with a modified wick technique. Microvasc Res 1977;14:27–36.
[34] Ley CD, Horsman MR, Kristjansen PEG. Early effects of combretastatin-A4 disodium phosphate on tumor perfusion and interstitial fluid pressure. Neoplasia 2007;9:108–12.
[35] Jain RK. Barriers to drug delivery in solid tumors. Sci Am 1994;271:42–9.
[36] Gulliksrud K, Brurberg KG, Rofstad EK. Dynamic contrast-enhanced magnetic resonance imaging of tumor interstitial fluid pressure. Radiother Oncol 2009;91:107–13.
[37] Kostourou V, Robinson SP, Whitley GSJ, Griffiths JR. Effects of overexpression of dimethylarginine dimethylaminohydrolase on tumor angiogenesis assessed by susceptibility magnetic resonance imaging. Cancer Res 2003;63:4960–6.
[38] Sonveaux P. Provascular strategy: Targeting functional adaptations of mature blood vessels in tumors to selectively influence the tumor vascular reactivity and improve cancer treatment. Radiother Oncol 2008;86:300–13.
[39] Tozer GM, Prise VE, Lewis G, Xie S, Wilson I, Hill SA. Nitric oxide synthase inhibition enhances the tumor vascular-damaging effects of combretastatin a-4 3-o-phosphate at clinically relevant doses. Clin Cancer Res 2009;15: 3781–90.
[40] Tozer GM, Kanthou C, Parkins CS, Hill SA. The biology of the combretastatins as tumour vascular targeting agents. Int J Exp Pathol 2002;83:21–38.
[41] Dowlati A, Robertson K, Cooney M, Petros WP, Stratford M, Jesberger J, et al. A phase I pharmacokinetic and translational study of the novel vascular targeting agent combretastatin a-4 phosphate on a single-dose intravenous schedule in patients with advanced cancer. Cancer Res 2002;62: 3408–16.
[42] Galbraith SM, Maxwell RJ, Lodge MA, Tozer GM, Wilson J, Taylor NJ, et al. Combretastatin A4 phosphate has tumor antivascular activity in rat and man as demonstrated by dynamic magnetic resonance imaging. J Clin Oncol 2003;21:2831–42.
[43] Stevenson JP, Rosen M, Sun W, Gallagher M, Haller DG, Vaughn D, et al. Phase I trial of the antivascular agent combretastatin A4 phosphate on a 5-day schedule to patients with cancer: Magnetic resonance imaging evidence for altered tumor blood flow. J Clin Oncol 2003;21:4428–38.